Query Sheet		
Journal Name: IJAT	Volume No. X	Issue No. Y

Article Name: Characteristics of the acoustic emission during horizontal single grit scratch tests: Part 1 characteristics and identification

Author Name: J. Griffin and X. Chen

Chapter No. Two (Part 1) Paginated S/W: Word

S.No.	Page No.	Query
1	7	Author: Please check equations below the line 'Cutting phenomenon occurs'.
2	9	Author: Boszar and Lorec (2006) has been changed to Boczar and Lorenc (2006) in the text as per the list. Please check.
3	17 (Ref)	Author: Mallat (1999) is given in the list but not cited in the text. Please check.

Characteristics of the acoustic emission during horizontal single grit scratch tests: Part 1 characteristics and identification

James Griffin and Xun Chen*

School of Mechanical, Materials and Manufacturing,
University of Nottingham,
Nottingham NG7 2RD, UK
E-mail: epzjg3@ad.nottingham.ac.uk
E-mail: x.chen@hud.ac.uk
*Corresponding author

Abstract: Material process in grinding involves three phenomena namely: rubbing, ploughing and cutting. Rubbing and ploughing, which usually occur before or after cutting, essentially mean the energy is being applied less efficiently in terms of material removal. It is therefore important to identify the effects of these different phenomena experienced during grinding. To identify the different phenomena, two channel Acoustic Emission (AE) signals were extracted by two AE sensors which would give verified energy information relating to the horizontal groove profile in terms of the material plastic deformation and material removal. With the use of a Fogale Photomap Profiler, accurate material surface profile measurements of the cut groove would be made and compared against the corresponding AE signal scratch hit data. A combination of filters, Short-Time Fourier Transform (STFT) would provide the salient components for comparison and classification of the three different levels of Single Grit (SG) processing phenomena. Verified classification was achieved from both Neural Networks and Fuzzy-c Genetic Algorithm Clustering Techniques and is discussed in the second part of this work.

Keywords: single grit scratch; Acoustic Emission; AE; feature extraction.

Reference to this paper should be made as follows: Griffin, J. and Chen, X. (XXXX) 'Characteristics of the acoustic emission during horizontal single grit scratch tests: Part 1 characteristics and identification', *Int. J. Abrasive Technology,* Vol. X, No. Y, pp.XXX–XXX.

Biographical notes: James Griffin completed his undergraduate studies in 1995 with a BEng from The University of Wales, College Cardiff. Between 1996 and 2003, he was a Member of the Defence Evaluation Research Agency (DERA) on numerous projects. One of that was significant used of Genetic Algorithms/Neural Networks to control an Unmanned Aircraft Vehicle (UAV). Whilst working for DERA/QinetiQ, he completed a second Degree BSc from Open University (1996–2001) in Technology biased towards Artificial Intelligence. He is now a PhD candidate within the Advanced Abrasive Technology Group at the University of Nottingham applying intelligent concepts to identify different grinding phenomena.

Xun Chen specialises in Advanced Manufacturing Technology including Application of Computer Science, Mechatronics and Artificial Intelligence to Broad Engineering Application. He has published more than 100 research papers. He is a founder Member of the International Committee of Abrasive

Technology. Before his employment at Nottingham, he was a Lecturer of Mechanical Engineering at the University of Dundee. He received his BEng from Fuzhou University. He received his MSc from Zhejiang University and his PhD from Liverpool John Moores University. He has been a visiting professor to Fuzhou University since 2001.

1 Introduction

Material particle displacements can be observed from the emitted elastic waves that propagate through material media (Royer and Dieulesaint, 2000) when an object is subjected to an external force. The released energy is primarily in the form of an Acoustic Emission (AE). From various stresses there are material particle displacements which are associated with AE and released in the form of material elastic energy. These elastic AE waves mimic the mechanical vibration of material and grit interaction and are extracted by AE sensors. Different AE characteristic signals are analogous to different external forces that act on the same material or the same force exerted on different materials (Chen et al., 2007; Griffin and Chen, 2006). Elastic waves can therefore be used for monitoring many machining processes and/or material non-destruction tests (Chen and Xue, 1999; Coman et al., 1999; Holford, 2000; Liu et al., 2005; Webster et al., 1994).

AE monitoring may be a difficult task; however, with correct data it is possible to monitor grinding phenomena features of interest. For example, such phenomena could be the level of burn or machine chatter marks or more importantly the efficiency of the grinding cut. The latter is of particular importance to this research in that Single Grit (SG) scratch experiments are important in the understanding of the microaspects endured during the grinding of workpiece materials. The aerospace alloys that have been the focus of this research are characteristically hard and heat resistive materials. For this paper horizontal scratch tests will be looked at using the CMSX4 material. Previous research (Chen et al., 2007; Griffin and Chen, 2006) looked at CMSX4 and other aerospace alloys however the focus was investigating rotating/radial scratch indented on two equally spaced workpieces (180° apart). With horizontal scratches the comparison between grinding wheel and SG scratch are more accurate as all the different levels of grinding phenomenon can be obtained whereas this is not the case with the rotating scratch tests. In this paper there is a focus on identifying the different levels of cutting phenomenon in grinding. It can be said that varying levels of SG interaction is an easier phenomenon to observe when compared to that of grinding. This is in terms of the distinguishing features between cutting, ploughing and rubbing and the irregular distribution of grains when interacting with the material workpiece. Once the observations and associated data has been achieved to distinguish between different features it can then be used to look at different levels of cutting, ploughing and rubbing experienced in a grinding. There has been a lot of work on SG analysis previous to this work where the material removal mechanisms were investigated from microscope analysis and acquired force signals (Hamed, 1977; Subhash et al., 2001; Wang and Subhash, 2002). This work looked at the different mechanics of grinding from different rake angles being presented during the scratch formation. In addition, such mechanisms such as the amount of Built-Up-Edge (BUE), material hardness and wheel speed increase the efficiency of grinding and decrease the surface roughness.

The AE wave is described as a non-stationary stochastic signal. AE extraction has been used in many machining processes from Milling, Drilling to Grinding where AE signals extracted from the material tests would traditionally use Root-Mean-Squared (RMS) level detection, event count, energy distributions, amplitude and the powers of dominate frequency bands (Chen et al., 2007). These techniques were broadly used and applied to general non-destructive condition monitoring tests based on events that were recorded in days instead of seconds. With SG scratch tests the different grinding phenomenon is produced by both short high-frequency and long low-frequency components. To that end, there is a need to use continuous recorded AE data and not that of event driven data initiated by the grit and workpiece touch interaction. For example, the interaction initiation is more likely to miss out key phenomenon from its delay response. The raw AE data is used for SG tests as RMS AE data can again miss out important information where high-frequency information is usually contained from the raw extracted AE data. To date little work has looked at the energy signatures experienced during SG scratch tests in grinding. However, this has been looked at in other areas of research such the characteristics of AE during single diamond scratching of granite (Clausen et al., 1996), where the RMS AE is extracted for different materials and different processes of rock cutting where the major mechanisms are microchipping, crack propagation and sliding friction. It could be said that microchipping, crack propagation and sliding friction for brittle materials are similar to ploughing, cutting and rubbing for ductile materials, respectively. The scratching of granite has many similarities with the scratching of alloys and in general, the higher the depth of cut made the more the peak AE amplitudes increase. For all the scratch tests carried out, the AE waveforms were normalised to 1 μm cut depths to compare like with like signals. In addition, for the grinding wheel tests the data was again normalised to 1 μm cut depth. SG scratching segregating different physical phenomenon through AE waveforms is a novel approach especially when applied to aerospace materials.

Using just the raw extracted time signal only gives the user one perspective of the AE properties. With Fast Fourier Transforms (FFTs) however, it is possible to get the frequency band components. The FFT estimates the frequency components as well as their associated amplitudes based on the trigonometric family functions (Smith, 1997). FFTs have been used for condition monitoring in the past albeit they do not give any time information of when the event occurred. This is fundamental to the very nature of spontaneously released transient elastic energy when materials undergo deformation or fracture or, a combination of both. FFT calculates the frequency average over the duration of the extracted signal and can be applied to a non-stationary AE signal, however, the results do not adequately describe the transient features in terms of frequency resolution (Li and Wu, 2000), instead FFT has to be used with a another technique that produces both the time and frequency band information.

With this weakness in mind there was a need for FFT to be represented in the time domain and this paved the way for Short-Time Fourier Transforms (STFTs). A similar function to FFT albeit the FFT is calculated for equally spaced time slots designated across the raw extracted time signal. There is a tradeoff between frequency and time resolution which is needed for accurately distinguishing SG features in a noisy environment. That said, and with the extra dimension of time, the STFT still offers a good solution when required to characterise an AE signal for SG scratches amongst other grinding phenomena.

Wavelet Packet Transforms (WPT) a family of orthogonal basis functions answers the tradeoffs between time and frequency resolution associated with STFT albeit to the detriment of computationally demanding algorithms. WPT represents the non-stationary signals through scaled time-frequency analysis. WPT provides both an approximate and a detailed representation of scaled time-frequency analysis with a high resolution at any point along the original time-frequency extracted signal (Chui, 1992). The scaled localised time-frequency analysis characterises AE signals in terms high-frequency burst of short duration and low-frequency components of longer duration (Li and Wu, 2000; Liu et al., 2005; Maradei et al., 2002; Staszewski and Holford, 2001).

In terms of capability the STFT is in between that of the Fourier Transforms (FTs) and WPT albeit there are subtle differences in why one technique is chosen over the other. STFT are constraint by the equally spaced window function used to obtain the time information with each time segment across the raw extracted time signal possessing frequency bands within the designated sensor frequency response range. With the STFT the more time resolution that is required the less frequency resolution is given and vice versa. If the tradeoffs between time and frequency resolution are respected and the signal has been extensively filtered in excess of machine and white noise then STFT is a quick and user friendly technique to use for classification. The WPT on the other hand breaks the signal up into smaller frequency components with high-short and low-long frequency components and the user is more able to read the exact point of phenomenon start or finish for a particular set frequency band. Therefore, the WPT resolution can be slightly better than that of STFT. Although WPT requires another technique to convert the Wavelet Packet Coefficients into frequency band components such as Hilbert Transforms, FFTs or even STFT and therefore is considered as both a time demanding and computationally expensive which is the reason why it was not chosen over STFT for the tests discussed in this paper.

The following equations display the differences between FT and STFT techniques (Strang and Nguyen, 1996):

$$X(f) = \int_{-\infty}^{\infty} x(t) \bullet e^{-2j\pi ft} \mathrm{d}t \tag{1}$$

where f is the frequency, t is the time, x denotes the signal under transform where $x(t)$ is the signal in the time domain and $X(f)$ is the signal in the frequency domain (FT of $x(t)$). Even though the transform is from $\pm\infty$ the FT computed function will sum up all the sine waves that are in a particular time step with a finite value (between sensor frequency response range), hence the function name: FFT. Next, the STFT will be introduced (Strang and Nguyen, 1996):

$$\mathrm{STFT}_x^{(\omega)}\left(t', f\right) = \int_{-\infty}^{\infty} \left[x(t) w^*\left(t - t'\right)\right] \bullet e^{-j\pi ft} \mathrm{d}t \tag{2}$$

as with Equation (1) $x(t)$ is the time domain signal under transform, $w(t)$ is the main difference from Equation (1) and is known as the window function and * is the complex conjugate. Based on the increment value of t', this will determine the resolution between the frequency and time domains (this is always chosen as a tradeoff between frequency and time domains). Essentially the STFT is the FFT multiplied by a discrete window function along the length of the original time domain signal.

The present investigation is motivated by the expectation that AE features of SG cuts can be extracted clearly by using STFT. Investigation and classification of such

waveforms provides a profound initial step in understanding and distinguishing the very fundamentals of grinding interaction which can ultimately increase the effectiveness of grinding monitoring. The main investigation objectives of this paper are:

- characterise the cutting, ploughing and rubbing phenomenon in horizontal SG scratch tests using material profile measurement techniques
- characterise the cutting, ploughing and rubbing phenomenon using the STFT of the AE gained from the horizontal SG scratch interaction
- verify those signals with Dual AE sensors set equal distances apart and from sensor delay determine the position of the scratch interaction
- normalise the signals for comparing like with like signals.

The investigations of SG horizontal scratch work in extracting AE waveforms to identify the energy footprints of cutting, ploughing and rubbing during conventional grinding is both novel and provides a different focus in obtaining efficient cutting conditions.

2 Experimental setup of horizontal SG scratch tests

The AE associated with grinding chip formation may be investigated by a scratch simulation of grinding. The experiment of SG scratch test was carried out on a specially designed rig fixed within a Makino A55 Machine Centre as shown in Figure 1. The aerospace alloy CMSX 4 was the chosen for the SG tests and all samples used were polished to a very high quality, which give the tests further confidence with respect to measurements. Roughness (R_a) across all workpieces were measured between 0.01 and 0.03 μm and were taken into consideration when calculating the groove cut area signifying whether rubbing, ploughing or cutting had occurred.

A SG was glued into a microscopic drilled hole of the specially designed steel plate. The steel plate would then be fixed to the spindle and rotated at the same range of commercial grinding speed. The SG was fixed to the plate in a protruding fashion which would ensure the SG was the 1st object to make contact with the workpiece when controlled within a micron of accuracy. The machine setup consisted of both the AE and force sensor being attached in a manner to ensure maximum signal extraction. To provide a sealed medium for the AE to vibrate from workpiece/SG to the sensor, grease was applied in between the AE sensor housing and workpiece holder rig. For monitoring the force and AE, two computers were synchronised by switch driven digital acquisition cards.

The scratch test was carried out by feeding a rotating Al_2O_3 grit towards a flat horizontally placed workpiece as illustrated in Figure 2. With a micron incremental grit stroke, a scratch groove will be formed on the surface of the flat sample. The average scratch depth is about 1 μm, which is a typical value of grinding chip in high efficiency grinding. The scratching wheel rotational speed is 4000 rpm with a feed rate of 4000 mm/min under down grinding condition. During a single scratch action the AE feature frequency bands/intensities change with respect to time. In short, the mechanical AE propagation should be considered in both time and frequency features. However, the prominent AE feature frequencies of the scratches are in the range 50–550 kHz, which are similar to the AE feature frequencies in grinding tests experienced in previous work (Chen et al., 2007).

Figure 1 Makino A55 grinding centre machine setup for horizontal SG scratch test (see online version for colours)

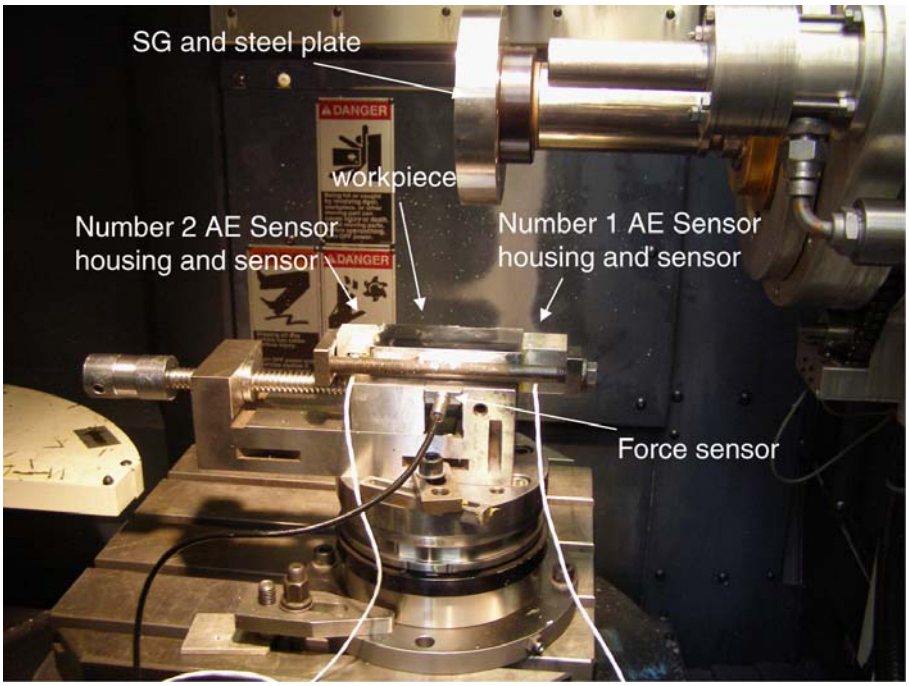

Figure 2 Sketch of horizontal SG scratch test rig

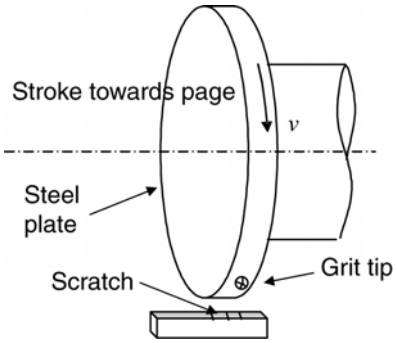

An AE data acquisition system where two Physical Acoustics WD AE sensors were used both identical and with a frequency response range at 100 kHz–1 MHz. The two sensors were setup equal distances apart (see Figure 1 for setup configuration). The sampling rate was set to 5 MHz to ensure no aliasing occurred when the signal was reconstructed using the Matlab Digital Signal Toolbox (DSP) and all the short burst high-frequency information was obtained. By using a Chebyshev Type II Infinite Impulse Response (IIR) band-pass filter with a cutoff frequency of 30 kHz–1 MHz most of the noise generated by the Makino A55 machine centre were eliminated at no great cost. In fact, the natural frequency (ω_n) of the machine was measured at 11 kHz was also eliminated from the extracted AE signals.

3 AE in SG scratch tests

When the process of grit to workpiece interaction occurs the AE is emitted as a material stress release process. This emitted AE during the scratch may come from elastic or plastic shear stress due to material removal or material deformation. It should also be noted that the AE intensities start the rise as the grit slightly interacts with the surface albeit touching but not causing any plastic deformation. This is rubbing without plastic deformation where the grit is close enough to comb across the surface but not so close that it leaves a mark. As the interaction of grit increased, it resulted in both elastic and plastic deformation where all three phenomena existed. The previous no mark contact and current continuous cut length were used for analysis of the rubbing, ploughing and cutting phenomena, respectively.

Different interactions were judged by measuring material profile. A Fogale Photomap Profiler was used to provide an accurate 3D measurement of the SG groove profile. The SG groove measurement analysis was obtained from 2D plan-view images and then an average cut over several stitched cuts would be used to make the phenomenon distinction. This profile cut was set against two observations (both cross section and cut direction profile measurements) to determine which phenomenon occurred out of rubbing, ploughing and cutting. The observation is based on the illustration of Figure 3. The following equation applies to Figure 3 to give a ratio for different phenomenon judgement:

$$M_{\text{ratio}} = \frac{A_{\text{surface}} + B_{\text{surface}} - \left(0.5R_{\text{a}}\,\text{width}\left(A_{\text{surface}} + B_{\text{surface}}\right)\right)}{C_{\text{surface}} - \leq \left(0.5R_{\text{a}}\,\text{width}\left(C_{\text{surface}}\right)\right)} \tag{3}$$

Where the areas A_{surface}, B_{surface} and C_{surface} are all calculated from using trapezoidal integration under a curve function (trapz, 2004). R_{a} is the surface roughness of the material at that measurement point, the width(A_{surface} + B_{surface}) is the profile cross section cut widths for A_{surface} and B_{surface}, the width(C_{surface}) is the width of the groove gap (distance in between A_{surface} and B_{surface}). Where A and B are the material deposits left behind from the SG groove being cut (C). With considering the specific surface roughness, the results of cutting, ploughing and rubbing have more confidence than if the specific surface roughness was not considered. The material profile cross section calculations were backed up with observations of the profile length of the direction of cut. This method would ensure a good confidence of the interaction phenomenon is found.

Looking at the illustration in Figure 3 and Equation (3):

Cutting phenomenon occurs, if

$$M_{\text{ratio}} < 0.9 = \frac{0.5R_{\text{a}}\,\text{width}\left(A_{\text{surface}} + B_{\text{surface}} + C_{\text{surface}}\right)}{A_{\text{surface}} + B_{\text{surface}} + C_{\text{surface}}} < 1$$

Ploughing phenomenon occurs, if

$$M_{\text{ratio}} > 1.1 = \frac{0.5R_{\text{a}}\,\text{width}\left(A_{\text{surface}} + B_{\text{surface}} + C_{\text{surface}}\right)}{A_{\text{surface}} + B_{\text{surface}} + C_{\text{surface}}} < 1$$

Rubbing phenomenon occurs, if

$$0.9 \leq M_{\text{ratio}} \leq 1.1 = \frac{0.5R_{\text{a}}\,\text{width}\left(A_{\text{surface}} + B_{\text{surface}} + C_{\text{surface}}\right)}{A_{\text{surface}} + B_{\text{surface}} + C_{\text{surface}}} \geq 1$$

where the width($A_{surface} + B_{surface} + C_{surface}$) is the profile cross section cut widths for $A_{surface}$, $B_{surface}$ and $C_{surface}$. The example displayed in Figure 3 illustrates the ploughing phenomenon as the $M_{ratio} = 6.904$. For illustration purposes both sides of the ploughed A and B regions represents the mean R_a (this may be considered over exaggerated in the figure) which for the discussed SG tests is 0.01 μm. The M_{ratio} and R_a term that is the extra parameter of equation along with M_{ratio} providing the distinction between the three phenomena is used to take the R_a into consideration when measuring the groove and ploughed BUE area, material measurements thus giving accurate material phenomenon results.

Figure 3 Displays an illustration of SG cut with ploughing phenomenon

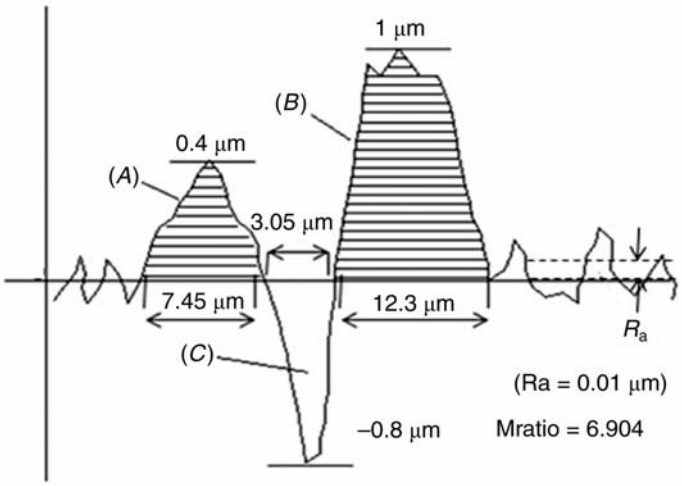

From looking at Equation (3) and the phenomenon boundary conditions it is possible to see that two factors will affect the value; the length of A, B and C; and the 0 line selection. In addition, extra ploughing materials might come from the ploughing materials being pushed forward by the grains; also the remained surface roughness from sample preparation might distort the profile which is considered in Figure 3, Equation (3) and its associated boundary phenomenon conditions.

The removal or non-removal of materials during SG scratch pass depends on the cutting action of grit to workpiece interaction. The groove is ideally created from a starting rubbing grit action followed by a ploughing/cut combination, then actual cut action followed by another ploughing/cut combination and then lastly, a rubbing action. Depending on the obtained cutting depth, the grit may experience rubbing, ploughing and cutting phenomenon that engages with the workpiece materials. The proportion of rubbing, ploughing or cutting in a grit pass depends on the amount of grit engagement between grit and workpiece material (quantified in terms of the material and groove area). The SG engagement can be displayed by the profile of the material groove cut, the measurement of the SG before and after the experiment and, the constant monitoring of first touch which is sensed by the calibrated AE sensor (set to 35 dB). It is also noted that the stress under the grit depends on the undeformed chip thickness. The larger the undeformed chip thickness, the higher the force needed to remove the chip. Therefore higher stresses would be initiated.

Figure 4 shows the AE signals of a SG scratch test (T212) from two AE sensors are almost the same. Both channels act as verification to one another displaying the SG phenomenon with confidence. Reference the phenomena displayed from the STFT representations of AE Hit 2 in Figure 4, the measured cut length were 401 µm. The interaction between grit and workpiece takes 14 µs calculated based on the following equation:

$$v_g = \frac{\pi D \mathrm{RPM} - v_w}{60} \tag{4}$$

where v_g is the grain cut through speed, wheel rotational speed rpm is 4000 rpm, the diameter D of the steel wheel on which the grit glued upon is 138 mm and the test piece feed speed v_w is 4000 mm/min. The calculation of v_g gives a very fast peripheral grain cut through speed of 28836 mm/s. Looking at Figure 4 again, the phenomena here took as long as 0.8 ms which is 50 times greater than the interaction between grit and workpiece. This phenomenon might be explained in that the physical stress prolonged with a delay response time due to the transitional process of the propagating wave excited from the workpiece to the pickup of the AE sensor. Therefore, the AE behaviour representing cutting, ploughing and rubbing phenomena is expanded in time. Pencil break tests (Barbezat et al., 2004; Boczar and Lorenc, 2006) also displayed a large response time to what can only be described as a microsecond fracture, Figure 4 displays this calibration phenomenon with a synchronised downward force signal (Fz). It can be seen the AE extracted pencil fracture is represented by a recorded 50 N force however the 50 N force is captured over a much longer time period which is representative of the applied force and not the actual fracture. Figure 4 displays the Hsu-Heilsen pencil break calibration method (Barbezat et al., 2004; Boczar and Lorenc, 2006) is an international standard where the breaking of a high polymer graphite pencil provides a localised AE burst which is analogous to broadband step-release transient wave. This extracted wave can be assumed as the amplitude and frequency response characteristic of the sensor. This method of AE sensor calibration has been used in grinding technologies before (Hwang et al., 2000).

To ensure there was a good segregation for the AE signals when presented to the classifier, parallel coordinates were used to show any cross over and potential misclassification. Each signal AE hit was normalised to a 1 µm cut signal therefore ensuring with deeper/shallower cuts there was no cross over from the designated ploughing and cutting signals.

Looking at Figure 5, it was noticed that the changing feature of the intensity of AE signals was similar to shape of grit scratch. Therefore, both amplitude of AE in time domain and the frequency band intensities could correlate to the material interaction characteristics identified as rubbing, ploughing, cutting, ploughing and then rubbing, though the AE wave response takes much longer than the actual mechanical interaction.

Under such assumptions, the grit to workpiece interaction and AE extracted signal are consistent for calculations. The signal albeit stretched is still representative of the scratch interaction and the three phenomena could still be located as long as careful scratch map measurements are taken and the correct ratio measurements are applied to the STFT representation.

Figure 4 Top: force and AE pencil break, middle: STFT, bottom: FFT slices of STFT

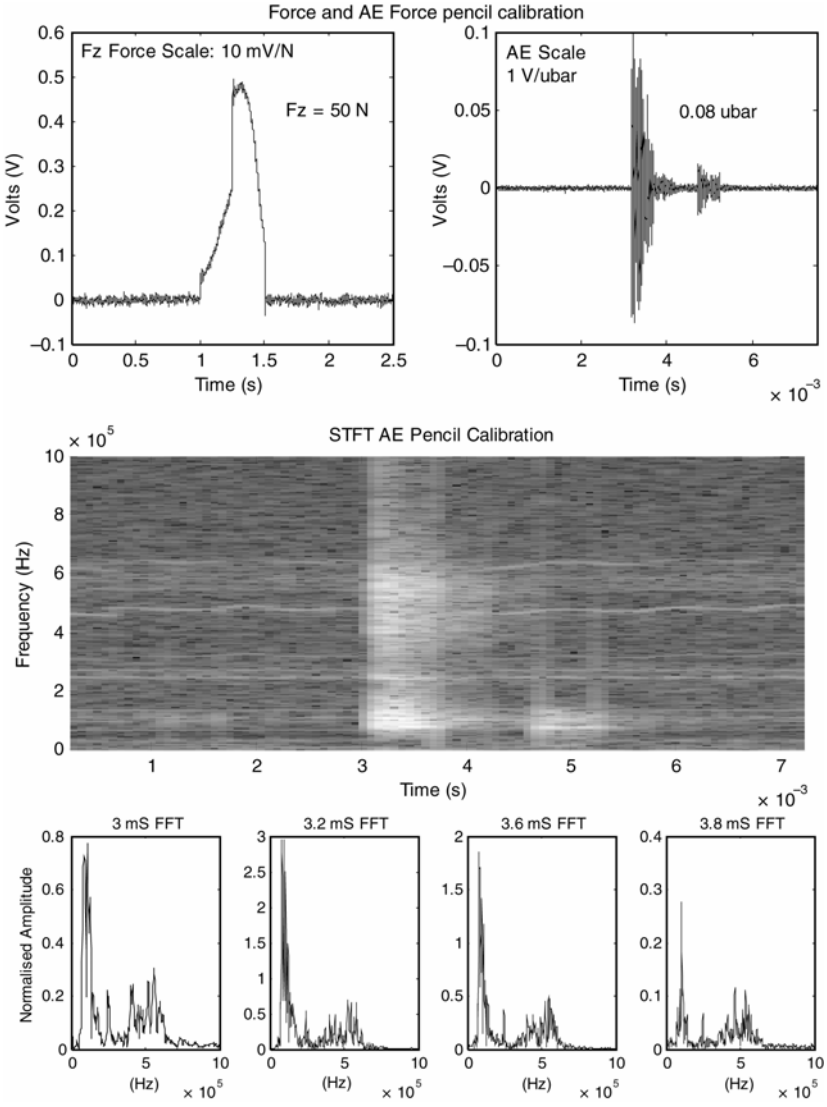

Figure 6 Top displays the STFT for SG4 T212 Hit 17. The middle of the figure represents the FFT slices obtained from the STFT thus relating to the horizontal cross section cut profiles (Figure 6 bottom) which signify whether the signal is cutting, ploughing or rubbing. Equation (4) was applied to material measurements along with general observations to decide the segregation of the identified phenomenon. For cutting phenomenon there are much higher amplitudes experienced than with ploughing and rubbing. All phenomena occupy the same peak frequency bands however the higher amplitudes are for cutting, then next, ploughing and lastly, in between the machine noise (normalised magnitude of 0.6) with a magnitude of 0.3 (it was found that the rubbing phenomenon has a damping effect on the noise extracted signal) to a magnitude of approximately 0.8 is the rubbing phenomenon.

Figure 5 Hit 2, top: raw extracted time signal, bottom: STFT

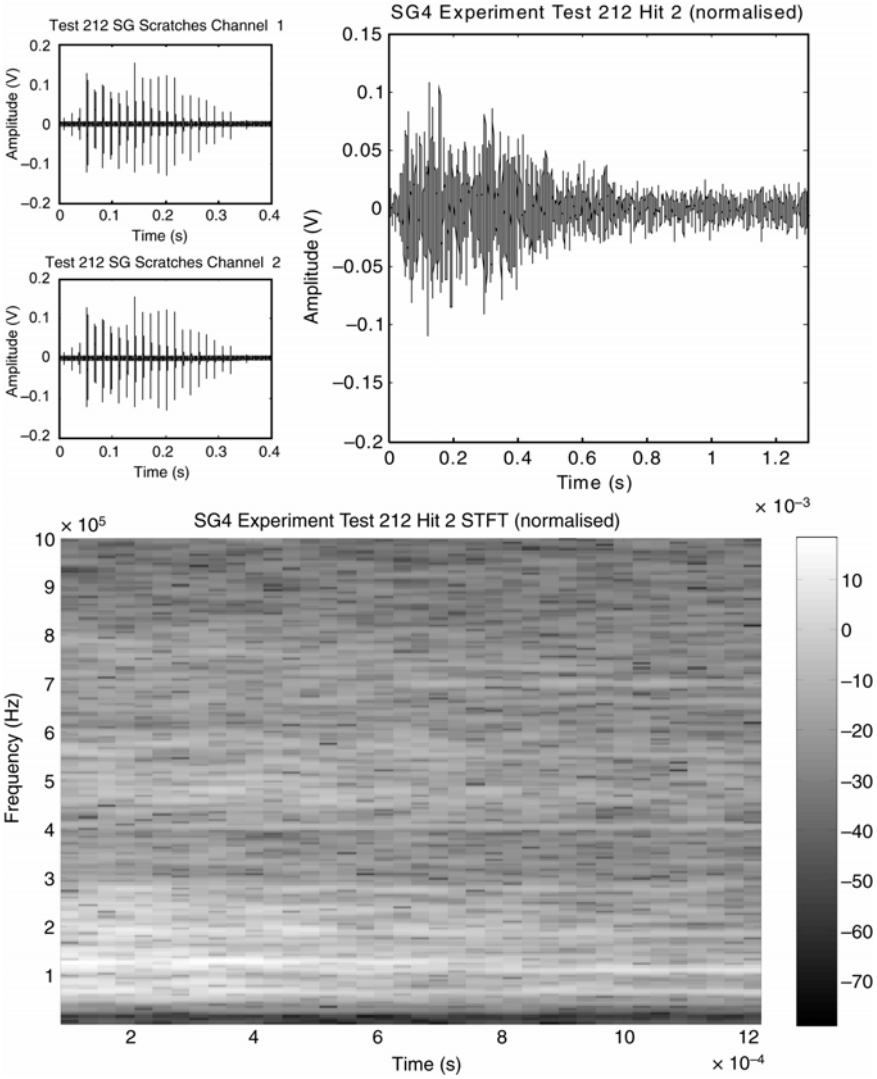

Note: Machine: Makino A55; SG Material: Al_2O_3; Workpiece: CMSX4; SG Dimensional depth and width appx. 1 μm; Dry down grinding: V_s = 4000 rpm; V_w = 4000 mm/min; a_p = 0.001 mm.

From those patterns ploughing occupied between 50 and 300 KHz of the major frequency band peaks. The normalised FFT magnitude was between 1 and 2 with side bands either side of the largest frequency band between 0.7 and 1.4 normalised magnitudes. Cutting also had similar major frequency band peaks between 50 and 300 KHz. The normalised magnitude for the major band peak was between 2.4 and 4 with side bands the same or slightly less than that of the ploughing side bands magnitudes. Both ploughing and cutting have slight frequency band peaks around the 500 KHz range and cutting has slightly larger peaks when compared with rubbing and ploughing at the 750 KHz range. Rubbing has major frequency bands between 30 and

500 KHz with the major peak ranging from 0.3 to 0.8 normalised magnitude. With rubbing there are a range of energy bands either side of the major peak frequency band which are half the magnitude of the major peak frequency band for rubbing.

Figure 6 SG4 Test 212 Hit 17 displays the STFT (Top) and FFT slices (Middle) and profiles relating to cutting, ploughing and rubbing phenomenon (bottom)

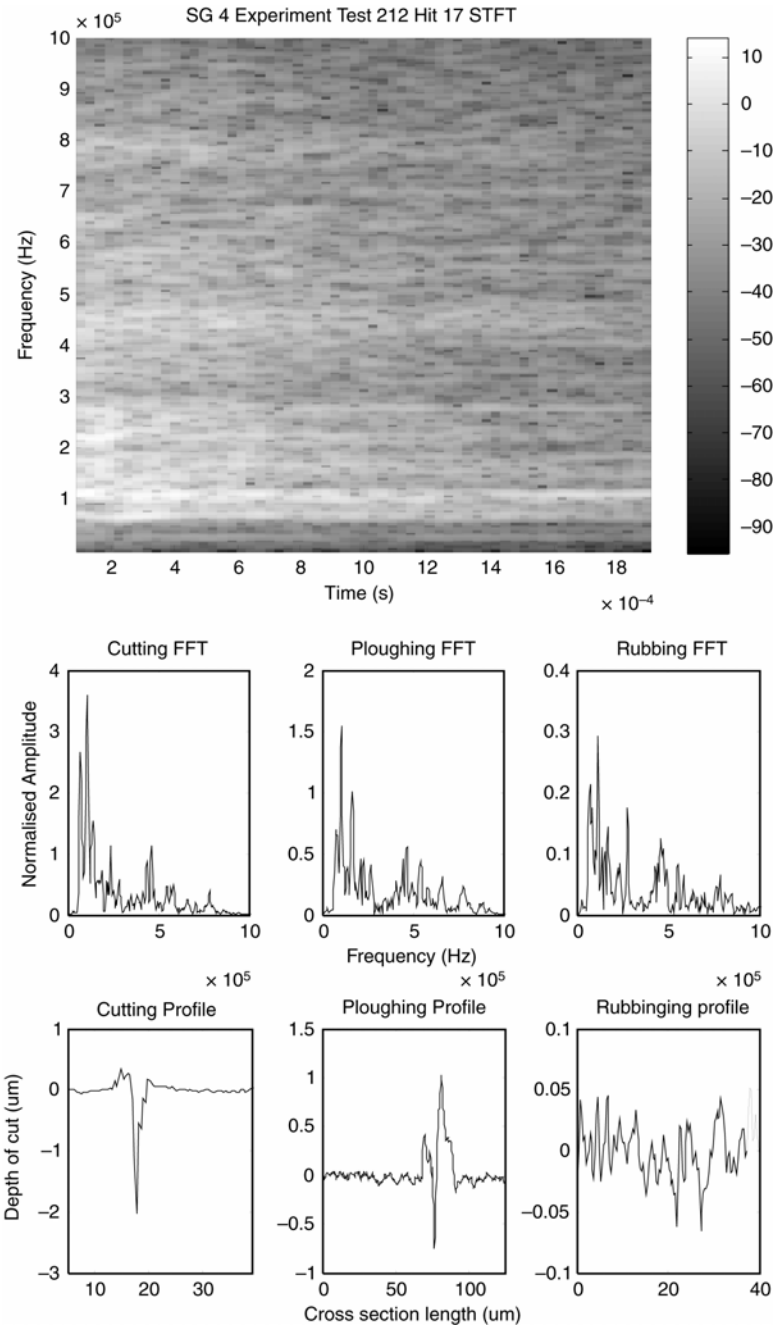

Figure 7 displays the AE signals of rubbing phenomena as there was no mark on the workpiece for the pass (Test T211) just before the next incremental machine pass (Test T212) which left scratch marks on the workpiece. The STFT analysis results shown in Figure 7 is similar to the rubbing features that shown in Figure 4. Note the scratch hit obtained for Test 212 contain all three phenomenon of cutting, ploughing and rubbing. Although most of the rubbing extracted signals came from Test 211 where 5 hits were extracted and no visible mark was made on the workpiece. This interaction gave good confidence of rubbing without plastic deformation.

Figure 7 Displays the hit before T212 contact (T211)

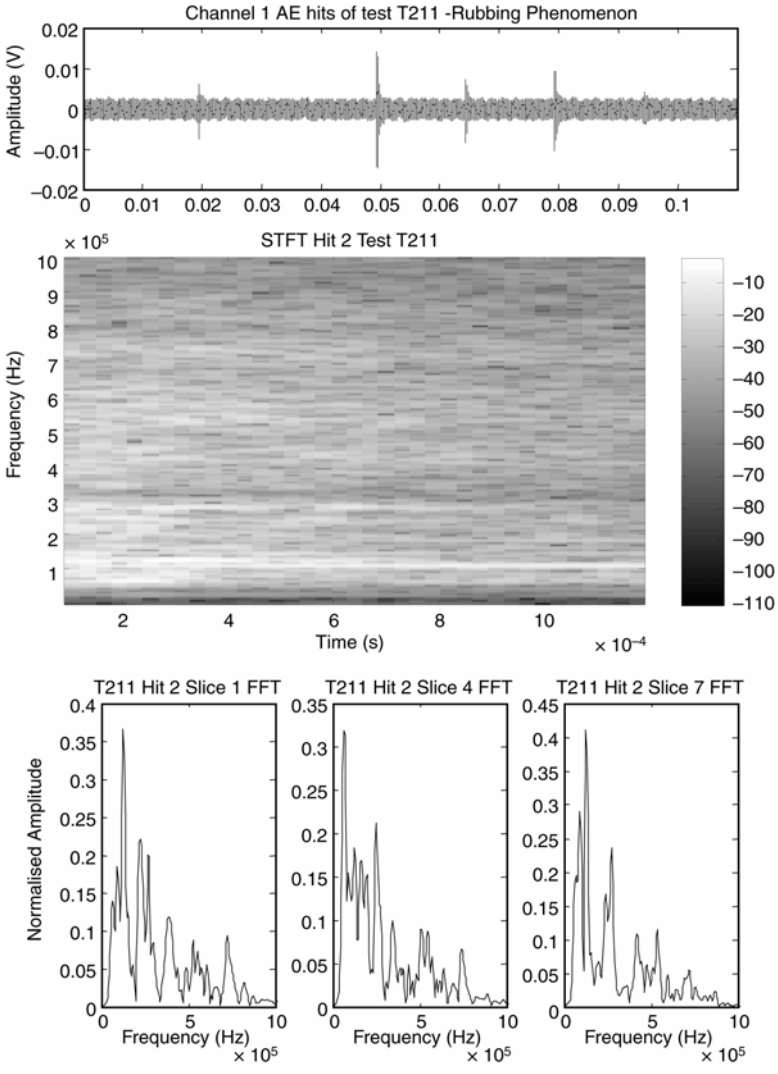

A STFT spectrum of the noise signal can be seen in Figure 8. The noise has represented frequency bands although the intensities are fairly low and they are clearly different from rubbing signal phenomenon.

Figure 8 Noise signal extracted at the end of Test 212

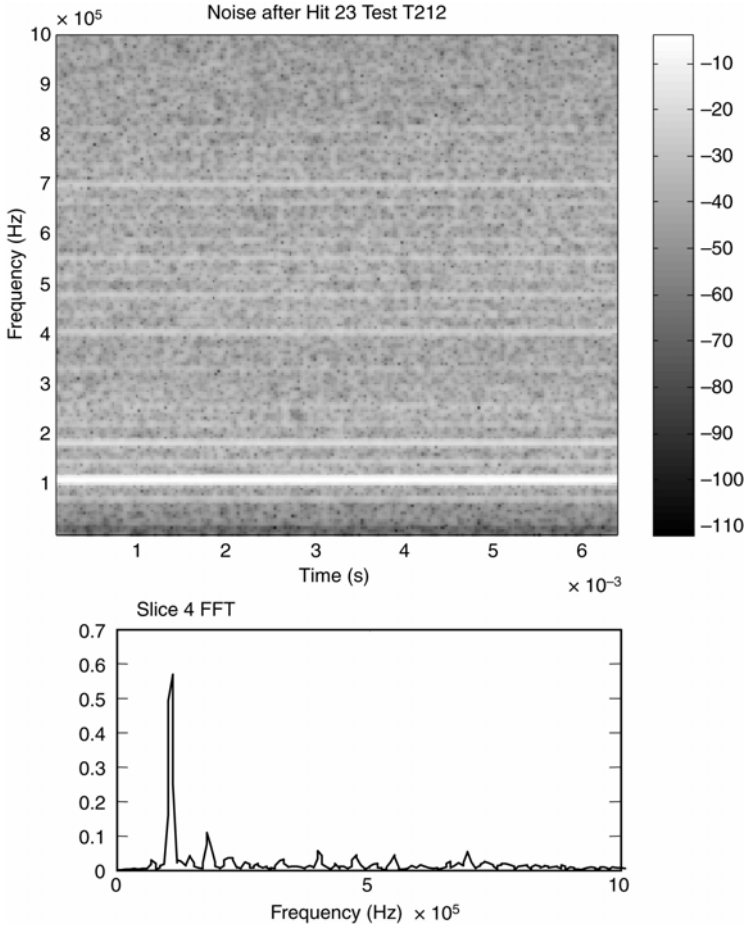

With the different energy signatures occurring from the SG interacting within the workpiece the STFT provide a good solution for separating the cutting, ploughing and rubbing phenomenon. Ploughing and cutting are somewhat similar in that the material is push/slide to one side or material removed, respectively; as these predominately cause material plastic deformation. The energy is consumed from surface deformation. In the rubbing case however there is surface friction (Kalpakjian and Schmid, 2003) this suggests therefore, that different AE signatures should be apparent between the two different phenomena. Rubbing does not remove or slide any material away, instead, it touches the surface with no visible markings which signifies elastic material characteristics in that the material deforms and returns back to its original state after a SG pass has occurred. In short, the boundaries are much closer in terms of AE distinguishing features of ploughing and cutting. Ploughing and cutting are perhaps the most difficult phenomenon to separate based on this assumption. The classification technique need to be as accurate as possible to ensure the sharpness of the waveforms are accurately represented when trying to distinguish the frictional energy and material deformation energy in the form of plastic or elastic energy.

All AE signals should be normalised to a standard level to avoid misclassification. For instance, if a measured 4 μm cut existed then the decibel level for that associated AE signal would be much stronger than the decibel level of an AE gained by a 1 μm cut. Here the decibel magnitude level of the AE for a 1 μm cut was taken as the basis throughout the tests. This is done by multiplying by a factor to ensure the level is in line with the 1 μm cut level. This normalisation is necessary as the AE gained from ploughing with a 4 μm cut has greater FFT magnitude intensities when compared with the AE gained from cutting within a 1 μm cut. Based on these different intensities from measured different depth of cuts it was deemed necessary to normalise the signal to then be able to compare like with like signals.

Figure 9 displays raw extracted time series AE signals that have not been normalised and have been normalised, respectively. Following on is the STFT representation before and after normalisation. Figure 9 Top left displays Hit 2 a non-AE normalised signal with a measured depth of cut of 0.25 μm. After the signal has been multiplied by a factor of 4 to bring it in line with a 1 μm cut (Bottom left) the new normalised signal is displayed at the top right of Figure 3. The bottom right displays the FFT vectors extracted from the STFT of Hit 2 before normalisation and after normalisation together with a STFT vector of Hit 4. The normalise FFT magnitudes are of similar levels and can be compared without causing a problem during segregation and classification. The normalisation would either be multiplied or divided by a factor amount to mimic the 1 μm signal extracted levels.

Figure 9 Normalisation of AE signal and cutting phenomenon FFTs after normalisation

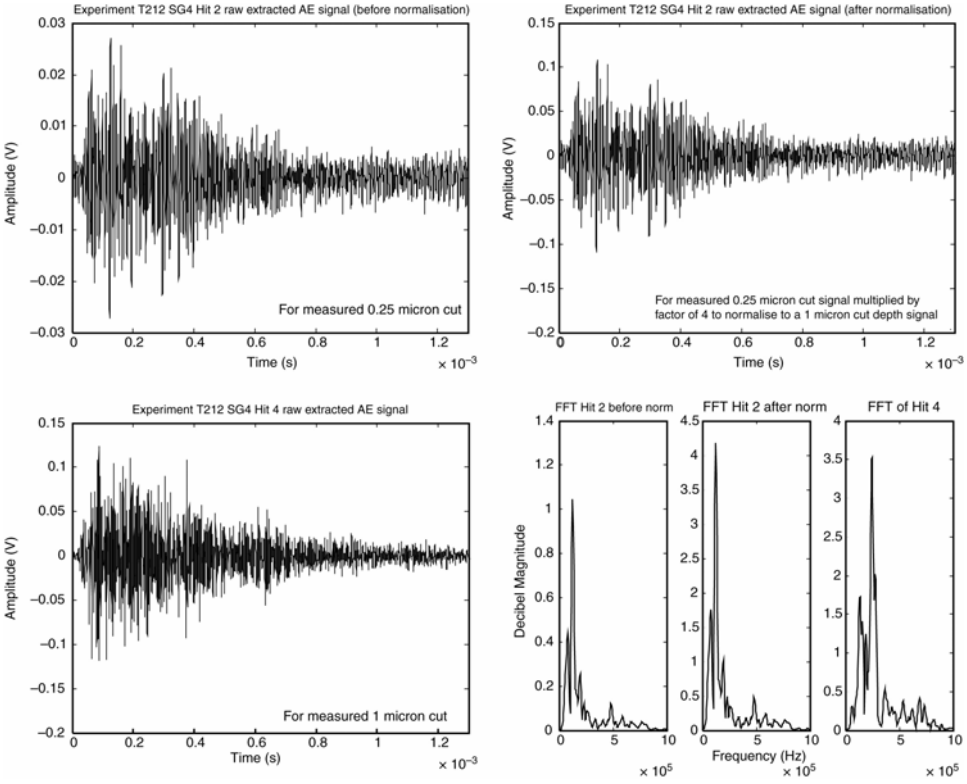

To verify and normalise the AE extracted signals, an AE pencil lead break test (Barbezat et al., 2004; Boczar and Lorenc, 2006) was used to ensure the AE sensors were calibrated on a daily basis during the tests. AE signal normalisation was only applied to plastic deformed phenomenon to ensure the segregation between cutting and ploughing phenomenon, with the rubbing phenomenon however this was not required.

4 Conclusive remarks

Identifying the fundamental signatures of SG interactive phenomenon is a key to the process of monitoring grinding; this paper is specifically concerned with the aerospace material CMSX4. Once the microscopic level of grinding activity has been identified and verified through a number of repeat tests it is then ready for identification of the macrolevel phenomenon (full grinding). This paper presents an investigation using AE signals to identify the SG phenomenon of cutting, ploughing and rubbing. The difficulty of using AE techniques for monitoring SG phenomenon is that AE signals are often weak and merged by other AE signals from other sources such as mechanical and white noise. The key point is how to distinguish the AE signals of relevant phenomenon from other AE signals.

This paper has demonstrated that STFT is a useful technique to distinguish the frequency bands occupied by cutting, ploughing and rubbing phenomena. The results show that AE energy for the three phenomena is concentrated between the frequency ranges of 30 kHz–1 MHz. Parallel coordinates were used to see the general patterns for cutting, ploughing and rubbing phenomena. From those patterns it was possible to see all three phenomena occupied between 50 and 500 KHz of the major frequency band peaks. Cutting had the most dominant peaks, then next, ploughing followed by rubbing.

Cutting and ploughing were difficult to distinguish due to their similar plastic material energy properties. Rubbing was difficult to distinguish from noise as the noise levels were in-between identified rubbing phenomenon. To that end, as the some rubbing cases consisted of noise it was thought the extra classification of noise would be confusing for the classifier and hinder the classifier accuracy. The rubbing phenomenon was seen to either, have slightly higher amplitudes than that of noise (occupies a wider range of frequency bands than that of noise) and in some cases having less magnitude than that of noise which was assumed due to the damping of the AE signal experienced in some rubbing cases. This is verified from the obtained AE hit data with no mark being present on the workpiece, the next 1 μm depth cut increment provided both the scratch hit phenomenon for cutting, ploughing and further rubbing. In the case of the scratch hit phenomenon the rubbing was determined from the AE time span covering more of a signal when compared with the actual distance travelled of the scratch groove (the surface here was very similar to the general roughness of the workpiece). The rubbing phenomenon is different from both cutting and ploughing phenomenon as it has only elastic deformation energy properties and ploughing/cutting has plastic deformation energy properties. With elastic deformation there should be no or very little marking on the workpiece.

References

Barbezat, M., Brunner, A.J., Flueler, P., Huber, C. and Kornmann, X. (2004) 'Acoustic emission sensor properties of active fibre composite elements compared with commercial acoustic emission sensors', *Sensors and Actuators*, Vol. 114, pp.13–20.

Boczar, T. and Lorenc, M. (2006) 'Time-frequency analysis of the calibrating signals generated in the Hsu-Nielsen system', *Physics and Chemistry of Solid State*, Vol. 7, No. 3, pp.585–588.

Chen, M. and Xue, B.Y. (1999) 'Study on acoustic emission in the grinding process automation', *American Society of Mechanical Engineers*, *Manufacturing Engineering Division, MED Manufacturing Science and Engineering (The ASME International Mechanical Engineering Congress and Exhibition)*, 14–19 November, Nashville, TN, USA, ASME, Fairfield, NJ, USA.

Chen, X., Griffin, J. and Liu, Q. (2007) 'Mechanical and thermal behaviours of grinding acoustic emission', *International Journal of Manufacturing Technology and Management (IJMTM)*, Vol. 12, Nos. 1–3, pp.184–199.

Chui, K.C. (1992) '*An Introduction to Wavelets*' San Diego: Academic Press, ISBN 91-58831.

Clausen, R., Wang, C.Y. and Meding, M. (1996) Characteristics of acoustic emission during single diamond scratching of granite', *Industrial Diamond Review*, Vol. 3, pp.96–99.

Coman, R., et al. (1999) 'Acoustic emission signal – an effective tool for monitoring the grinding process', *Abrasives*, December/January, p.5.

Griffin, J. and Chen, X. (2006) 'Classification of the acoustic emission signals of rubbing, ploughing and cutting during single grit scratch tests', *International Journal of Nanomanufacturing*, Vol. 1, No. 2, p.1

Hamed, M.S. (1977) 'Grinding mechanics – single grit approach,' PhD Thesis, Leicester Polytechnic.

Holford, K.M. (2000) 'Acoustic emission – basic principles and future directions', *Strain*, Vol. 36, No. 2, pp.51–54.

Hwang, T.W., Whitenton, E.P., Hsu, N.N., Blessing, G.V. and Evans, C.J. (2000) 'Acoustic emission monitoring of high speed grinding of silicon nitride', *Ultrasonics*, Vol. 38, pp.614–619.

Kalpakjian, S. and Schmid, S.R. (2003) *Manufacturing Process for Engineering Materials*, Prentice Hall, ISBN 0-13-040871-9, pp.510–520.

Li, X. and Wu, J. (2000) 'Wavelet analysis of acoustic emission signals in boring', *Proceedings of the Institution of Mechanical Engineers*, *Part B: Journal of Engineering Manufacture*, Vol. 214, No. 5, pp.421–424.

Liu, Q., Chen, X. and Gindy, N. (2005) 'Fuzzy pattern recognition of AE signals for grinding burn', *International Journal of Machine Tools and Manufacture*, Vol. 45, Nos. 7–8, pp.811–818.

Mallat, S.G. (1999) *A Wavelet Tour of Signal Processing*, 2nd edition, San Diego, London: Academic Press.

Maradei, C., et al. (2002) 'Monitoring of the tool condition with acoustic emission signal analysis using wavelet packets', *Insight: Non-Destructive Testing and Condition Monitoring*, Vol. 44, No. 12, pp.786–791.

Royer, D. and Dieulesaint, E. (2000) *Elastic Waves in Solids I, II*, New York: Springer-Verlag Berlin Heidelberg.

Smith, S.W. (1997) *The Scientist and Engineer's Guide to Digital Signal Processing*, California Technical Publishing, ISBN 0-9660176-3-3.

Staszewski, W.J. and Holford, K.M. (2001) 'Wavelet signal processing of acoustic emission data', *Key Engineering Materials*, Vols. 204–205, pp.351–358.

Strang, G. and Nguyen, T. (1996) *Wavelets and Filter Banks*, Wesley Cambridge Press, ISBN 0-9614088-7-1, pp.1–29, 61–68.

Subhash, G., Loukus, J.E. and Pandit, S.M. (2001) 'Application of data dependent systems approach for evaluation of fracture modes during single-grit scratching', *Mechanics of Materials*, Vol. 34, pp.25–42.

Trapezoidal function *(trapz)* (2004) Matlab Function Reference, Vol. 3, P – Z, *Version 7, The Mathworks Inc.*, pp.2–2286.

Wang, H. and Subhash, G. (2002) 'An approximate upper bound approach for single-grit rotating scratch with a conical tool on pure metal', *Wear*, Vol. 252, pp.911–933.

Webster, J., Marinescu, I. and Bennett, R. (1994) 'Acoustic emission for process control and monitoring of surface integrity during grinding', *Annals of CIRP*, Vol. 43, No. 1, pp.299–304.